# Numerical Flutter Simulation -Application to Structural Design of Main Surface of SST Experimental Aircraft-

Jiro NAKAMICHI[*1] and Hamid Reza KHEIRANDISH[*2]

[1]National Aerospace Laboratory, Tokyo, Japan jiro@nal.go.jp
[2]Research Center of Computational Mechanics, Inc, Tokyo, Japan hamid@rccm.co.jp

## Introduction

The estimation of flutter boundary of high-speed aircraft plays an essential role in the structural design concepts and parameters. Its role gets more importance in the case of supersonic transport because relatively thin wing-sections or control surfaces are necessarily used for these configurations. Therefore an interactive relation between design parameters and flutter boundary suggested by experiment or CFD is highly requested at primarily steps of structural design. With remarkable progresses in computing speed and numerical methods, the CFD is now of much current interest to do this request. Linear methods can predict the flutter boundary with relatively high accuracy in all the flows except for transonic region where the flow is highly nonlinear or when the flow is highly separated. In these regions the nonlinear methods should be employed for accurate prediction.

The authors have developed a CFD Code to numerically simulate unsteady coupled fluid-structure problems based on Navier-Stokes/Euler equations. This code has been used and verified in several large scale problems such as 3-D high aspect ratio wings[1,2], and Arrow wing configuration[3]. This report describes numerical simulation of aeroelastic responses of the NAL Supersonic Transport(SST) experimental aircraft around transonic region. The unsteady Euler equations coupled with structural equations were solved to obtain flutter boundary of SST. The results were obtained either with and without structural damping and were compared with linear theory results when available. The aileron flutter, like the linear theory, was found the most critical one for this configuration. The flutter boundaries are estimated lower than those obtained by the linear theory for the range of Mach number 0.6-1.0

## Governing Equations

The computation is based on unsteady Euler equations for governing flow field and a modal approach form of equations for structural side(Eqs. 1). These equations can be described in non-dimensional form as

$$\frac{\partial \hat{Q}}{\partial t}+\frac{\partial \hat{F}}{\partial \xi}+\frac{\partial \hat{G}}{\partial \eta}+\frac{\partial \hat{E}}{\partial \zeta}=0$$

$$m_i\ddot{q}_i + k_i^2 m_i q_i = \bar{Q}\iint_S\left(-C_p n_z\right)\Phi_i\, dS \qquad (1)$$

where $q_i$ are generalized coordinates: $\Phi_i$, $m_i$ and $k_i$ are the natural modes, generalized masses and natural reduced frequencies corresponding to the i'th mode, respectively. $\bar{Q}$ is the nondimensionalized dynamic pressure and $n_z$ is the z-direction component of normal vector to the wing surface. The double integration symbol implies the integration over the whole aircraft surface. The structural equations of motion are derived by the assumption that the deformation of the body under consideration can be described by superposing the orthogonal natural vibration modes weighted with generalized displacements. For more information on obtaining governing equations see Ref 4-5. The integration of governing equations are implemented using a second order upwind TVD scheme[6,7] for the flow equations and Wilson's $\theta$ implicit method[8] for the structural ones. The procedure of unsteady computations can be carried out as follows:

1. Compute steady state solution at a given Mach number
2. Assume dynamic pressure
3. Assume initial value for some of generalized velocities
4. Solve structural equations and update surface geometry and corresponding surfaces and internal grids
5. Update flow field solution
6. Repeat steps 4 and 5 for many cycles and save time history of generalized coordinates.

To find flutter boundary at a given Mach number, repeat steps 3 to 6 for a range of dynamic pressures and find stable and unstable regions by analyzing mode responses.

## Characteristics of Experimental Model

A plan-view of this model is given in Figure 1. The dimensions and typical parameters of the are as follows; Fuselage length 11.5m, wing root chord-length 4.2m, span length 4.72m, aspect ratio 2.1. Swept-back angles of inner and outer boards are 24° and 28.8°. The structural dynamic characteristics, natural mode shapes and frequencies of this model were found, using NASTRAN, by FHI. The flutter boundary, except at transonic regions, was also determined using linear theory. They found that the aileron flutter is the most critical one. The first 24 symmetric and anti-symmetric modes of fuselage and wings are shown in Table 1. The modes which contain aileron motion are marked by '*'.

[1]Head, Aeroelasticity, Structures Division
[2]Senior Eng., Technical Development

Table 1. Vibration Characteristic of Experimental Model

| Mode No. | Frequency Hz | Dominant Mode Shape |
|---|---|---|
| 1 | 0.0 | Rigid Pitching |
| 2 | 0.0 | Rigid Heaving |
| 3 | 0.0 | Rigid Rolling |
| *4 | 8.7 | FLoB, WB |
| 5 | 11.5 | FLaB |
| *6 | 16.5 | WB-s |
| *7 | 26.0 | FLoB, Aileron T-s |
| *8 | 27.4 | WB-s |
| *9 | 29.8 | Aileron T-s |
| 10 | 30.2 | Aileron T-s |
| 11 | 34.1 | FLaB |
| 12 | 38.1 | FLaB T |
| 13 | 42.4 | V |
| 14 | 42.9 | FLoB |
| 15 | 47.7 | H-a |
| 16 | 48.7 | H-s |
| 17 | 56.3 | W-s |
| 18 | 62.5 | W-a |
| 19 | 67.9 | W-s |
| 20 | 71.0 | W-a, V |
| 21 | 72.2 | W-s, Aileron B |
| 22 | 76.9 | W-s, Aileron T |
| 23 | 83.0 | V |
| 24 | 89.1 | V |

F:Fuselage W:Main Surface H:Horizontal Tail V:Vertucal Tail
B:Bending T:Torsion
Lo: Longitudinal La: Lateral -s :Symmetric -a: Anti-symmetric
* Mode indicated in Figures

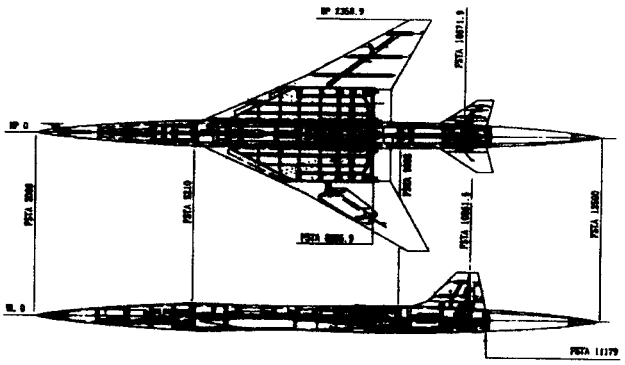

Fig 1. Plan-View of SST Experimental Model

The flight envelope of SST experimental aircraft in a frame of Altitude vs. Equivalent Air Speed (EAS) is illustrated in figure 2. This figure shows the rocket launching path and also free flight path. Our objective is to investigate that the flight path is free of flutter especially in transonic region.

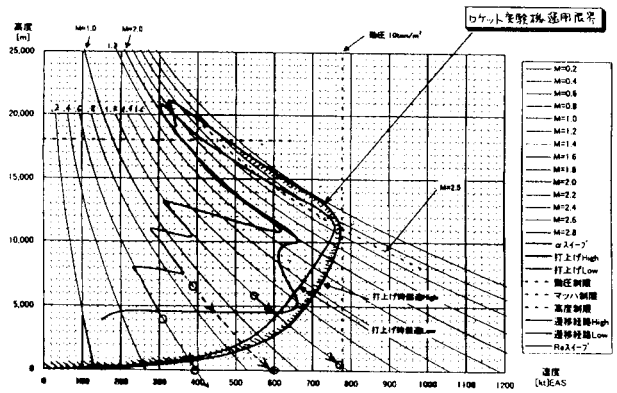

Fig 2. Flight Envelope of SST

**Numerical Results and Discussions**

A H-H type mesh with 126x121x80 grid points was generated around full SST configuration for these computations. The mesh generator is based on elliptic methods. The minimum size of grid in normal direction is of order of .005 based on the wing root chord length. The outer boundaries are put at least 15 times the wing root chord length away from the surfaces in the stream-wise and normal directions and 3 times the half-span length in span-wise direction. A schematic view of grids around the half-span of SST is shown in Fig 3.

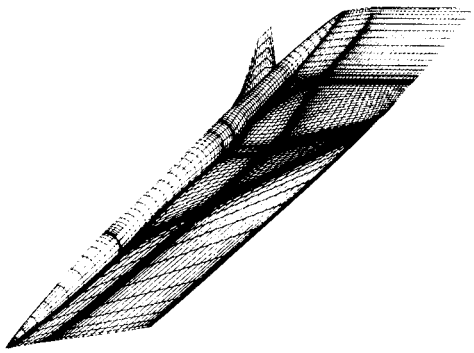

Fig 3. Grid Distributions on SST

The first 24 modes, which were found by NASTRAN, were considered in the computations. These modes contain symmetric modes as well as anti-symmetric modes. The SST responses in Mach number range 0.6 to 1.2 at several dynamic pressures with or without structural damping were found. The results are illustrated as selected generalized modes(dominant modes) vs. non-dimensional time at each Mach number and dynamic pressure to investigate the SST responses. For the sake of convenience modes marked by "*" in table 1 are only illustrated in this paper. They are mode 4: fuselage and main surface bending, mode 6: main surface symmetric bending, mode 7: fuselage bending and aileron torsion-symmetric, mode8: main surface bending-anti-symmetric, and mode 9: aileron torsion-anti-symmetric modes. The first three rigid modes are not considered here.

An example of steady state pressure distributions on four different semi-span stations(0.0%, 30%, 50%, 70%) at Mach number 0.9, obtained by present computation and linear theory, are given in Figure 4. The 0.0% semi-span stations, corresponds to body-symmetric line.

Hereunder unsteady numerical computation results will be shown and discussed. At all the numerical simulations, structural damping is set to 0.0 unless mentioned.

The results at Mach number 0.6, where dynamic pressures are 100kPa and 80kPa, respectively are given in figures 5-6. This figures show the time histories of some dominant generalized coordinates. It can be seen from figure 6 that only those modes which contain aileron mode(ie; mode7 and 8) will be diverged first by a 20kPa increase in dynamic pressure. Other modes show positive damping at this range of dynamic pressure.

Figure 7-9 show simulation results at Mach number 0.9. The dynamic pressures are set at 90kPa, 60kPa and 25kPa. At this Mach number simulations with structural damping equal to 0.02 were also carried out. These results are given in figures 10-11. As the previous case, modes 7 and 8 are the modes which show instability first by an increase in dynamic pressure. The inclination is similar for the case with structural damping 0.02, too. The critical dynamic pressure( the dynamic pressure at which flutter occurs) is about less than 60kPa without structural damping while it increases to 70kPa when structural damping is 0.02.

The SST response at Mach number 1.0 and dynamic pressure 90kPa is shown in figure 12. The modes 7 and 8 are already diverged at this dynamic pressure. Other modes are still show convergence.

The results at Mach number 1.2, dynamic pressures 130kPa and 100kPa are given in figures 13-14. The response is stable at 100kPa while some modes(ie; mode 7 and 8) seems to be unstable at 130kPa. The tendency of modes are similar to the previous cases..

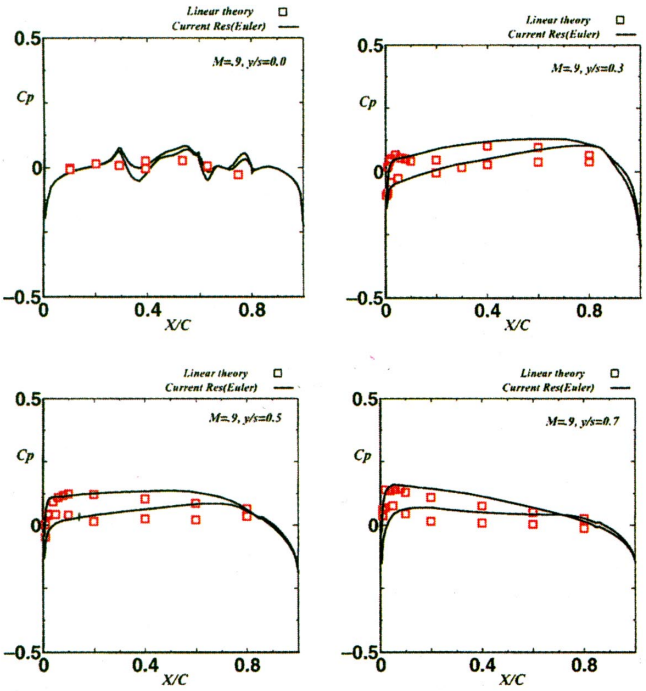


Fig 4. Steady State Pressure Distributions, M=.9, A=0.0

Figure 15 shows the main surface flutter boundary obtained by present method and linear-theory. The vertical and horizontal axes are: equivalent air speed(EAS) and Mach number, respectively. In this figure main surface and aileron flutter boundaries obtained by linear theory are illustrated by dashed line. The triangles show the data computed by present method. The results are agreed together only at Mach number 1.2. The flutter speed obtained by present simulations are lower than those estimated by linear-theory for Mach numbers less than 0.9 A dip-like curve is obtained by present method although no shock waves were seen in all the computations.

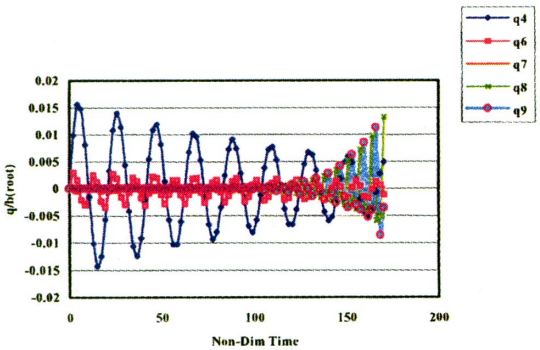


**Fig.5 SST Response at Dp=100kPa, M=0.6**

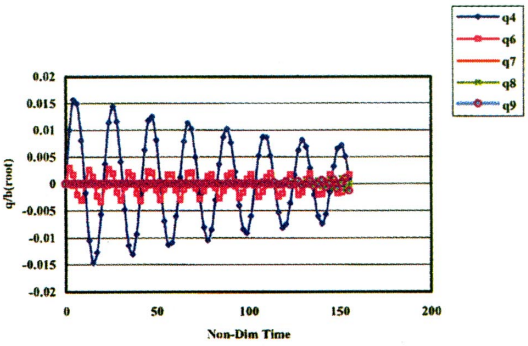


**Fig.6 SST Response at Dp=80kPa, M=0.6**

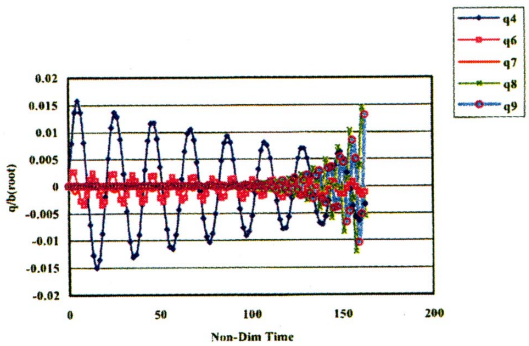


**Fig. 7 SST Response at Dp=90kPa, M=0.9**

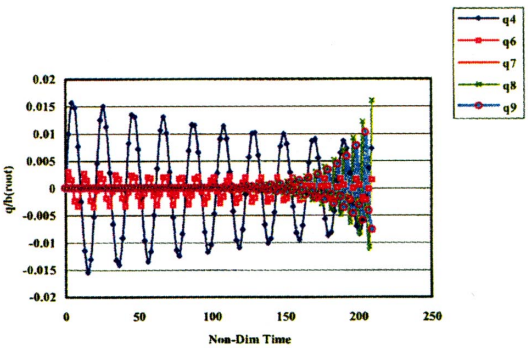


**Fig. 8 SST Response at Dp=60kPa, M=0.9**

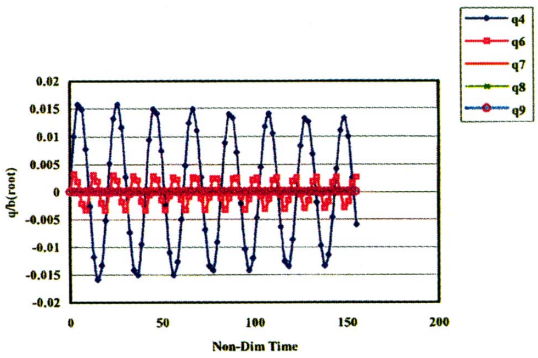


**Fig.9 SST Response at Dp=25kPa, M=0.9**

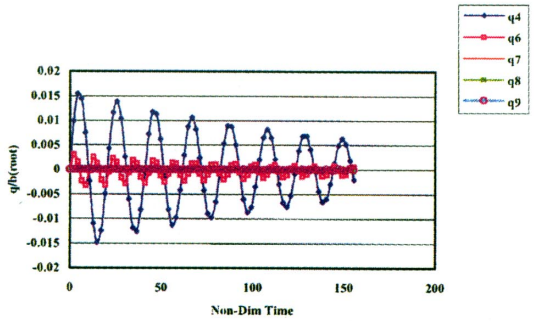


Fig.10 SST Response at Dp=60kPa, M=0.9, g=.02

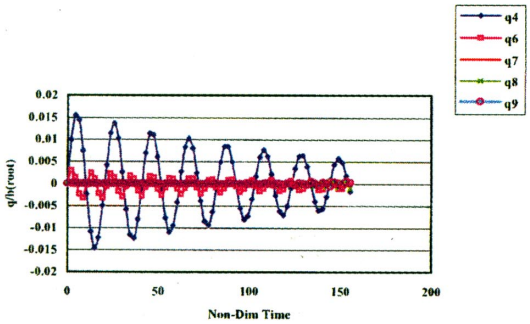


Fig. 11 SST Response at Dp=70kPa, M=0.9, g=.02

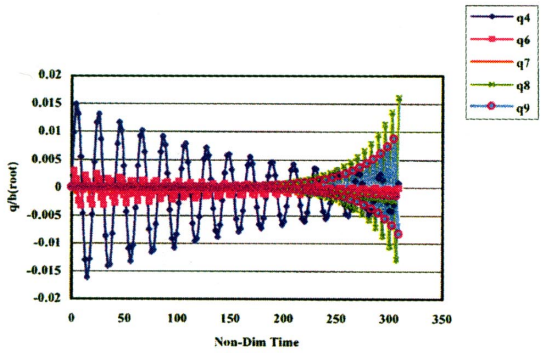


Fig. 12 SST Response at Dp=90kPa, M=1.0

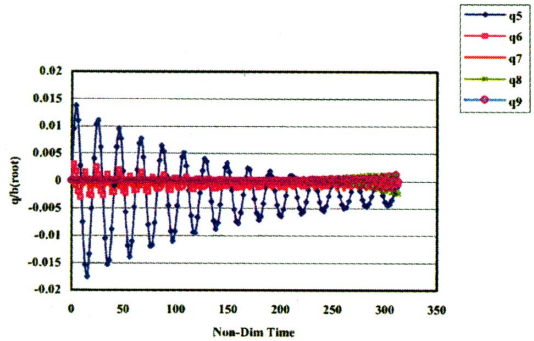


Fig. 13 SST Response at Dp=130kPa, M=1.2

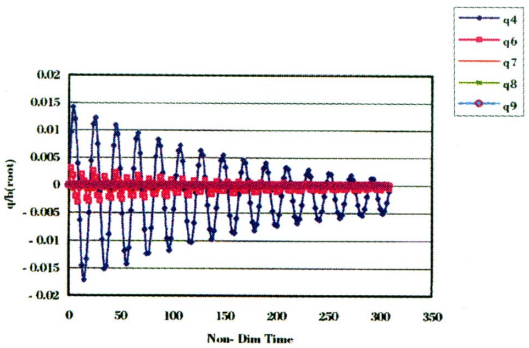


Fig.14 SST Response at Dp=100kPa, M=1.2

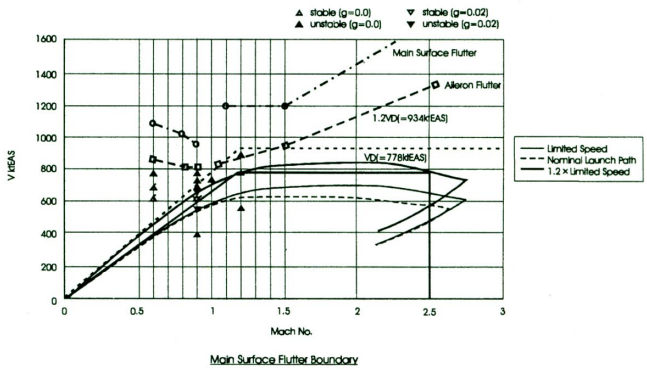


Main Surface Flutter Boundary

Fig 15. Main surfaces Flutter Boundaries

## Conclusion

Numerical flutter simulation of full-SST configuration has been carried out using Euler solution at transonic region. The aileron flutter was found as the most critical one. The flutter speeds obtained by the present code do not agree well with those of linear-theory except at Mach number 1.2.

The authors thank Fuji Heavy Industries for their offering the results of vibration analysis for the present studies.

## REFERENCES

[1] H. Kheirandish, G. Beppu and J. Nakamichi, Numerical Simulation if Viscous Unsteady Flow around Wings Oscillation in Elastic Modes, JSCES Symposium, Tokyo, Japan (1996)

[2] H. Kheirandish, G. Beppu and J. Nakamichi, Computational Investigation of Wings Flutter To be published in" International Journal of Computational Fluid Dynamics, 99/10

[3] H. Kheirandish, and J. Nakamichi, Inter-Code Validation between NAL and DLR in the Aeroelastic Simulation for SST Configuration, CEAS/ICAS/AIAA/NASA Langley International forum on Aeroelasticity and structural Dynamics( Virginia-Williamsburg), 1999/6/21-25

[4] T.H. Pulliam and J.L. Steger, Recent Improvements in Efficiency, Accuracy, and Convergence for Implicit Approximate Factorization Algorithms, AIAA Paper 85-0360, (1985)

[5] R.L. Bisplinhoff, H. Ashley, Principles of Aeroelasticity, Dover Pubns (1975)

[6] H. Yee and A. Harten, Implicit TVD Schemes for Hyperbolic Conservation Law in Curvilinear Coordinates, AIAA paper 85-1513 also AIAA Journal, Vol.25, No.2,(1987), pp.266-274

[7] H. Yee and G.H. Klopfer and J.L. Montagne, High-Resolution Shock-Capturing Schemes for Inviscid and Viscous Hypersonic Flows, NASA TM-100097 (1988).

[8] K.J. Bate and E.L. Wilson, Numerical Methods in Finite Element Analysis, Prentic-Hall (1976)